Label-free and naked eye detection of PNA/DNA hybridization using enhancement of gold nanoparticles†

Sang Kyu Kim,[ab] Hyunmin Cho,[ab] Jinyoung Jeong,[ab] Ji Na Kwon,[ab] Yongwon Jung[ab] and Bong Hyun Chung*[ab]

Received (in Cambridge, UK) 22nd December 2009, Accepted 5th March 2010
First published as an Advance Article on the web 1st April 2010
DOI: 10.1039/b926940a

Utilizing a gold enhancement process after inducing electrostatic interaction between positively charged gold nanoparticles and negatively charged target DNA hybridized to neutral PNA capture probes, a new method for label-free detection of DNA was developed and successfully applied to detect H5-type DNA.

The detection of DNA is important in analysis of DNA sequences, genomic research, and early diagnosis for cancer. Therefore, various methods for detecting DNA based on electrical, optical, and mechanical strategies have been developed.[1–4] Among those methods, optical methods, especially fluorescent techniques, have generally been used, due to high sensitivity and easy accessibility to commercialized equipment. The fluorescent method, however, requires an expensive detection system and additional steps to label analytes with fluorophores. The labeling steps increase cost and complexity of reactions and are therefore not suitable for rapid detection.

Recently, various substitutes for the fluorescent technique have been developed.[5–7] One of the most interesting approaches for detecting DNA was demonstrated by Mirkin and coworkers.[5] Gold nanoparticle probes and synthetic oligonucleotide targets were cohybridized to capture DNA-immobilized substrates, and a signal amplification process employing the silver enhancement process allowed the target-bound spots to be visible. In a similar sense, Alexandre *et al.*[6] used biotinylated target DNA and gold-conjugated streptavidin instead of a gold-conjugated DNA probe. The subsequent silver precipitation process enabled the targeted spots to be visible. These methods allowed target DNA to be detected in low concentrations by either the naked eye or with a flat-scanner (so-called scanometric detection) without expensive detection systems. Although this method could be an alternative to the fluorescent technique,[5–9] it still requires the process for making conjugates between gold nanoparticles and DNAs.

Here, we introduce a new method for label-free scanometric detection of DNA that utilizes the electrostatic interactions between positively charged gold nanoparticles and negatively charged DNA bound to neutral peptide nucleic acid (PNA) capture probes. The following gold enhancement process enabled the targeted spots to be visible because positively charged gold nanoparticles specifically bound to the targeted spot. In this work, we could detect a synthetic oligonucleotide derived from an H5-type bird influenza virus, using both the naked eye and an optical scanner. As a consequence, it was observed that the sensitivity of this method was comparable to that of conventional fluorescent technique. It is greatly expected that this method can be used as a novel platform technology for detecting DNA in a convenient and cost-effective manner.

The DNA detection strategy and chip preparation are schematically illustrated in Fig. 1. The neutral PNA capture probes and the blocking materials were covalently immobilized on the transparent slide glass by EDC/NHS coupling. The hybridization between the target DNA and the capture probe PNA resulted in a negatively charged surface, due to the negative phosphate backbone of the target DNA. When the positively charged gold nanoparticles were introduced onto the slide, selective binding events between the nanoparticles and the DNA allowed the formation of gold/DNA composites through electrostatic interactions.[10–14] Finally, to visualize the nanoparticles bound to the DNA with the naked eye or an optical scanner, a signal amplification process was employed using a metal enhancement solution composed of metal ions and reducing agent. When metal nanoparticles, such as gold or silver nanoparticles, are treated with the metal enhancement solution, the gold or silver ions from the solution are catalytically deposited onto the metal nanoparticle, causing the nanoparticle to grow in size.[5] This process enabled the target DNA to be visualized by the naked eye or an optical scanner.

To create a positive charge on the nanoparticle surface, gold nanoparticles were coated with cetyltrimethylammonium bromide (CTAB), a cationic surfactant. Initially, the bare gold nanoparticles represented a negative zeta potential because the particles were stabilized by citric acid. However, when a CTAB solution was added into the citrate solution containing the gold nanoparticles, the zeta potential value became positive (see Table S2 in the ESI†). It appears that the CTAB molecules might surround the nanoparticles *via* an electrostatic interaction between the negatively charged citric acid on the particle surface and the positively charged ammonium ions in CTAB or *via* the exchange of a stabilizing agent from citric acid to CTAB, due to the relatively high concentration of

[a] *BioNanotechnology Research Center, Korea Research Institute of Bioscience and Biotechnology, P.O. Box 115, Yuseong, Daejeon 305-600, Republic of Korea. E-mail: chungbh@kribb.re.kr; Fax: +82-42-879-8594; Tel: +82-42-860-4442*
[b] *School of Engineering, University of Science and Technology (UST), P.O. Box 115, Yuseong, Daejeon 305-600, Republic of Korea*

† Electronic supplementary information (ESI) available: Materials and methods and supplementary data. See DOI: 10.1039/b926940a

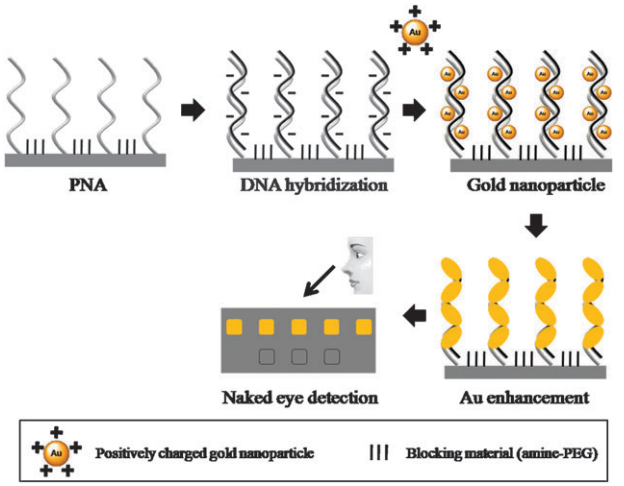

Fig. 1 Schematic diagram of DNA detection strategy by the naked eye or an optical scanner.

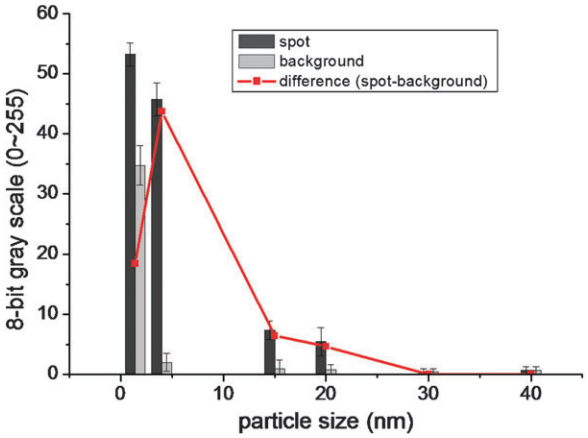

Fig. 2 Comparison of the grayscale response for various gold nanoparticle sizes (1.4, 4, 15, 20, 30, and 40 nm). The optimal particle size was 4 nm, resulting in the highest net difference between the spot and background.

CTAB compared to that of citric acid. Finally, PBST solution was added to the nanoparticle solution to create a similar hybridization condition. The zeta potential value slightly decreased due to an exchange of the negatively charged phosphate ions in PBST buffer for the positive ions from CTAB.

In fact, it is known that the critical micelle concentration (CMC) of CTAB is *ca.* 1 mM.[15] This means that micelles are formed in CTAB solution at a concentration greater than 1 mM. To test whether the positive zeta potential of the final solution containing the gold nanoparticles was caused by micelles in the CTAB, the zeta potential of the same solution without the nanoparticles was investigated. In the 0.2 M CTAB, the zeta potential value was greater than 35 mV (Table S4 in the ESI†), which was due to the formation of positively charged micelles from the CTAB at a higher concentration than in the CMC. However, the zeta potential of the solution (containing citrate, CTAB, and PBST) without the nanoparticles was 0.55 ± 1.42 mV (Table S4 in the ESI†), *i.e.* almost neutral. In that solution, it appears that the micelles from CTAB might be denatured by the negative ions from the citrate, various ions and surfactant (Tween20) in the PBST. This result indicates that the positive zeta potential value of the solution containing the nanoparticles was not due to the micelles from the CTAB, but rather to the CTAB-coated gold nanoparticles.

We investigated the effect of individual gold nanoparticle diameters (1.4, 4, 15, 20, 30, and 40 nm) on the 10 nM target DNA hybridized substrates, to find the optimal diameter for the positively charged gold nanoparticles. The optical responses were obtained in the form of 8-bit grayscale values using an optical scanner (white: 0–black: 255). As shown in Fig. 2, the results indicate that the smaller particles exhibited a stronger response than the larger particles. In a similar sense, Fang *et al.*[10] studied the effects of individual particle size on electrical responses. In their study, the small particles (5 ± 1 nm) demonstrated a stronger response than the larger particles (13 ± 2 nm or 20 ± 3 nm). In our experiment, the strongest response was observed with 1.4 nm gold nanoparticles with a gray level of 53.24. For the two largest particles (30 and 40 nm), no differences in intensity between the spot and the background were detected because they were thoroughly washed out. It is postulated that a small particle has better accessibility to the space between target DNAs than a large particle, and thus small particles strongly bind to the targeted spot.[10]

While 1.4 nm gold nanoparticles exhibited the strongest intensity, with a gray level of 53.24, they also caused a strong background signal (34.77), resulting in small differences in grayscale (18.47) between the spot and background. It appears that even though intensive washings were conducted several times, 1.4 nm nanoparticles were too small and reactive to wash out because they were strongly, nonspecifically adsorbed in the entire chip surface. It is noted that the highest difference in intensity (gray level: 43.74) between the spot and background was observed in a 4 nm gold nanoparticle, suggesting that this is the optimal diameter. It appears that a 4 nm particle has optimal accessibility and reactivity for specifically binding to targeted spots and less nonspecificity at the control spot. The 4 nm gold nanoparticles were therefore selected for the following experiments.

For the quantitative and qualitative DNA assays, the slide surface was modified by spotting PNA probes A and B using a commercial microarrayer, as shown in Fig. 3A. To test whether target DNA specifically hybridized with the probe PNA, a 10 nM Cy3-labeled target (A′) was incubated on the slide. Specific binding between the target A′ and the probe A was clearly observed (Fig. 3B). When the solution containing the 4 nm positively charged gold nanoparticles was introduced to the slide, the nanoparticles were specifically bound to the negatively charged hybridized spot while the gold nanoparticle did not bind to the non-complementary PNA probe.

To make the targeted spot visible, it was necessary to enlarge the gold nanoparticle bound to the target DNA through a metal enhancement process. In this experiment, we used a gold enhancement solution rather than a silver enhancement solution.[5] Gold enhancement solution provides several advantages, such as insensitivity to pH, lower background, and compatibility with physiological buffers, while silver irreversibly

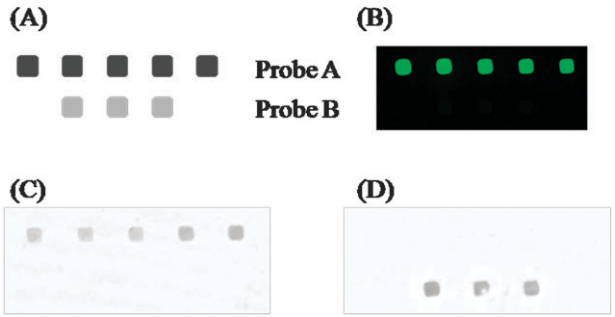

Fig. 3 (A) The slide glass was spotted with PNA probes A and B. (B) Fluorescent images of DNA chips with a 10 nM Cy3-labeled target A′. (C) Optical scanner image of a 10 nM target A (18-mer) hybridized DNA chip. The intensity of the grayscale value was *ca.* 49. (D) Scanner image of a 10 nM target B (50-mer) hybridized DNA chip, showing a stronger response, with a grayscale value of *ca.* 64.

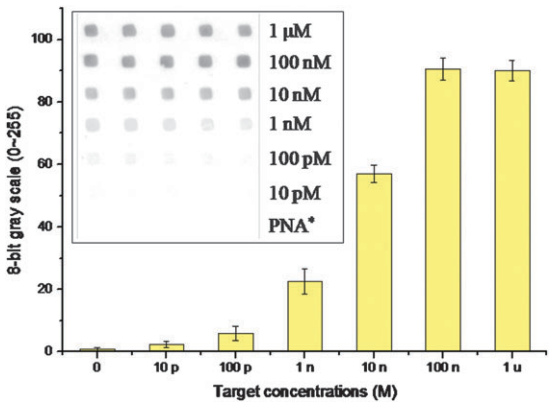

Fig. 4 Graph of 8-bit grayscale values depending on the concentration of target A. The concentrations of target DNA, from bottom to top, were 0, 0.01, 0.1, 1, 10, 100, and 1000 nM. The gray level increased with increasing target concentration. Inset: optical scanner images of different target concentrations. (*Only PNA probe without hybridization).

precipitates with chloride ion. Using gold enhancement solution, we also obtained superb results (spot signals), which improve on those obtained with silver enhancement (data not shown).[16] With the gold nanoparticles magnified by the gold enhancement process, the DNA spots became visible to the naked eye or an optical scanner. In the presence of non-complementary DNA, the spot became almost invisible, indicating that there was no nonspecific interaction between the positively charged gold nanoparticles and the neutral PNA probes (Fig. 3C and D). We also investigated the effect of target base length on the response and obtained the 8-bit grayscale values (white: 0–black: 255) using an optical scanner. With the same concentration of 10 nM target DNA, target A (18-mer) and target B (50-mer) gave gray levels of *ca.* 49 and 64, respectively, suggesting that the longer target DNA allowed for the capture of more positively charged nanoparticles and the generation of stronger responses (Fig. 3C and D).

The responses due to the various target concentrations (target A) were further explored by studying the gray levels of the targeted spots. Grayscale values were proportionally increased depending upon the target concentration, because more target DNAs could capture more gold nanoparticles. Fig. 4 shows that the intensity of gray levels is dependent on the concentration of target A (ranging from 10 pM to 1 μM), while the gray levels of PNA probe spots show almost zero values. The gray level increased from the detection limit of 10 pM to the saturation point of 100 nM of target DNA. The inset shows the optical scanner images of different target concentrations. This result is comparable to that obtained using the fluorescence method (Fig. S2 in the ESI†). Our method can also detect a 96-mer target DNA mimic, originated from influenza A virus (H5N1) segment 4 hemagglutinin (HA) gene, in the presence of excess non-related DNA/RNA mixture (Fig. S5 in the ESI†).

In this study, we demonstrated a new method for the label-free detection of DNA using the gold enhancement process after inducing the electrostatic interaction between the positively charged gold nanoparticles and the negatively charged target DNA hybridized to the neutral PNA capture probes. Among the various sizes of gold nanoparticles, 4 nm gold nanoparticles were found to exhibit the optimal response. In this method, the target-bound spot can be visualized by the naked eye or by using a commercialized optical grayscale flat-scanner. The grayscale levels were proportional to the concentration of the target DNA within the range of 10 pM to 100 nM, exhibiting comparable sensitivity to the fluorescence method. It is expected that this novel method offers the potential for label-free DNA detection in a cost-effective manner.

This work was supported by the Fundamental R&D Program for Core Technology of Materials funded by the Ministry of Knowledge Economy and a grant from the KRIBB Initiative Research Program (KRIBB, Korea), Republic of Korea.

Notes and references

1 S. J. Park, T. A. Taton and C. A. Mirkin, *Science*, 2002, **295**, 1503–1506.
2 Y. Fan, X. Chen, A. D. Trigg, C.-h. Tung, J. Kong and Z. Gao, *J. Am. Chem. Soc.*, 2007, **129**, 5437–5443.
3 J. Fritz, M. K. Baller, H. P. Lang, H. Rothuizen, P. Vettiger, E. Meyer, H.-J. Güntherodt, C. Gerber and J. K. Gimzewski, *Science*, 2000, **288**, 316–318.
4 D. Yao, F. Yu, J. Kim, J. Scholz, P. Nielsen, E. Sinner and W. Knoll, *Nucleic Acids Res.*, 2004, **32**, e177.
5 T. A. Taton, C. A. Mirkin and R. L. Letsinger, *Science*, 2000, **289**, 1757–1760.
6 I. Alexandre, S. Hamels, S. Dufour, J. Collet, N. Zammatteo, F. De Longueville, J. L. Gala and J. Remacle, *Anal. Biochem.*, 2001, **295**, 1–8.
7 Y. C. Cao, R. Jin and C. A. Mirkin, *Science*, 2002, **297**, 1536–1540.
8 R. Moller, R. Powell, J. Hainfeld and W. Fritzsche, *Nano Lett.*, 2005, **5**, 1475–1482.
9 J. K. Pokorski, J. M. Nam, R. A. Vega, C. A. Mirkin and D. H. Appella, *Chem. Commun.*, 2005, 2101–2103.
10 C. Fang, Y. Fan, J. Kong, Z. Gao and N. Balasubramanian, *Anal. Chem.*, 2008, **80**, 9387–9394.
11 Jie Zhang, Boon Ping Ting, Nikhil R. Jana, Zhiqiang Gao and Jackie Y. Ying, *Small*, 2009, **5**, 1414–1417.
12 T. Kodama, A. Jain and K. Goodson, *Nano Lett.*, 2009, **9**, 2005–2009.
13 L. Fabris, M. Dante, G. Braun, S. Lee, N. Reich, M. Moskovits, T. Nguyen and G. Bazan, *J. Am. Chem. Soc.*, 2007, **129**, 6086–6087.
14 A. Ongaro, F. Griffin, L. Nagle, D. Iacopino, R. Eritja and D. Fitzmaurice, *Adv. Mater.*, 2004, **16**, 1799–1803.
15 H. Gao, R. Zhu, X. Yang, S. Mao, S. Zhao, J. Yu and Y. Du, *J. Colloid Interface Sci.*, 2004, **273**, 626–631.
16 D. Kim, W. L. Daniel and C. A. Mirkin, *Anal. Chem.*, 2009, **81**, 9183–9187.